



Search for AMSB with the DELPHI data

PRELIMINARY

T. Alderweireld¹, P. Johansson², A. Lipniacka², S. Paiano³, A. Perrotta³

¹ Faculté des Sciences, Université de l'Etat Mons, Mons, Belgium

² Fysikum, Stockholm University, Box 6730, S-113 85 Stockholm, Sweden

³ Dipartimento di Fisica, Università di Bologna and INFN, Bologna, Italy

Abstract

The data collected by the DELPHI experiment up to the highest LEP2 energies were used to put constraints on the Anomaly Mediated SUSY Breaking model with a flavour independent m_0 parameter. The experimental searches covered several possible signatures experimentally accessible at LEP, with either the neutralino, the sneutrino or the stau being the LSP. They included the search for nearly mass degenerate chargino and neutralino (always present in AMSB), the search for Standard Model like or invisible Higgs boson, the search for stable staus, and the search for cascade decays resulting in the LSP (neutralino or sneutrino) and a low multiplicity final state containing neutrinos.

1 Introduction

After many years of searches in the collider experiments, there is still no evidence of the existence of supersymmetric particles. There are indeed several theoretical motivations to believe that nature must be supersymmetric and that the so far negative results of the searches can only set constraints on the spectrum of the SUSY particles and on the parameters of the model. The mechanism of SUSY breaking itself is still unclear. In the gravity mediated scenario (SUGRA) [1], SUSY gets broken in a hidden sector and the breaking is transmitted gravitationally to the observable sector. This mechanism is elegant, since it only requires already existing fields and interactions (like gravity). It suffers however from the so called SUSY flavour problem, that is the minimal version of SUGRA (mSUGRA) requires a large amount of fine tuning to avoid unobserved large Flavour Changing Neutral Current effects.

To cope with the SUSY flavour problem, different breaking mechanisms have been inspected. In the Gauge Mediated SUSY Breaking scenario (GMSB) [2] the breaking is transmitted via gauge forces. This model originates a very characteristic mass spectrum, with a light gravitino as the Lightest Supersymmetric Particle (LSP) and typically long lived NLSP's.

Anomaly Mediated Supersymmetry Breaking (AMSB) [3, 4] is another interesting solution to the flavour problem of mSUGRA. Rescaling anomalies in the supergravity lagrangian always gives rise to soft mass parameters in the observable sector. It follows that anomalies contribute to the SUSY breaking in any case, whatever is the symmetry breaking mechanism. We'll refer to AMSB as the model in which all other components that mediate the SUSY breaking are suppressed, and the anomaly mediation is the dominant mechanism.

AMSB is very predictive: all the low energy phenomenology can be derived by adding to the Standard Model (SM) just two extra parameters and one sign. Unfortunately, the minimal AMSB model results in tachyonic masses for sleptons at the electroweak scale. One way of getting rid of tachyons is to suppose additional, non anomaly, contributions to the SUSY breaking which can generate a positive contribution to the soft masses squared. There are few string motivated solutions that generate such positive contribution without spoiling the RG invariance of the soft terms. In most cases, such contribution is universal for all sfermion masses and, in practice, it is enough to add just one extra parameter to the model. This arises, for instance, when the visible and the hidden sectors lie in separate 3-branes that communicate only through gravitation [3]. There are other solutions [5] that lead to flavour dependent mass terms; such possibilities are less predictive (since the sfermion spectrum depends on more parameters) and they will not be investigated further in this paper. However, the characteristic gaugino spectrum of AMSB is the same also for those models, and many of the considerations that follow can be applied also to them.

2 Phenomenology of AMSB

If there is only one common squared mass term for all scalars, all masses and couplings can be derived in terms of just three parameters and one sign:

- the mass of the gravitino, $m_{3/2}$;
- the ratio of the vacuum expectation values, $\tan\beta$;

- the common scalar mass parameter m_0 .
- the sign of the Higgs term, $sign(\mu)$.

In this context, m_0 can even be considered as a phenomenological term that parameterizes the lack of knowledge of the method with which the sleptons acquire physical masses.

Low energy gaugino masses, scalar masses and trilinear couplings in AMSB are given by:

$$M_i = \frac{\beta_g}{g} m_{3/2} \quad (1)$$

$$M_{\tilde{Q}}^2 = -\frac{1}{4} \left(\frac{\partial \gamma}{\partial g} \beta_g + \frac{\partial \gamma}{\partial y} \beta_y \right) m_{3/2}^2 + m_0^2 \quad (2)$$

$$A_y = -\frac{\beta_y}{y} m_{3/2} \quad (3)$$

where g are the gauge couplings, y the Yukawa couplings and γ and β are renormalization group functions. This soft mass spectrum has distinctive features [4] which differ from the usual SUGRA or GMSB scenarios.

- The gravitino is heavy (and this has several advantages for the cosmology).
- The ratios of gaugino masses at the electroweak scale are determined by the ratios of the corresponding β functions. Therefore, they assume in a natural way different values with respect to the theories with gaugino mass unification at GUT:

$$M_1 : M_2 : M_3 \simeq 2.8 : 1 : -8.3 \quad (4)$$

These ratios have been computed by including the largest next to leading corrections [4]. Typical values of μ allowed by the model imply $M_2 < M_1 < |\mu|$. The chargino and neutralino mass eigenstates are therefore well approximated by either pure gaugino and pure higgsino states, with $M_{\tilde{\chi}_1^0} \sim M_{\tilde{\chi}_1^\pm} \sim M_2$, $M_{\tilde{\chi}_2^0} \sim M_1$, $M_{\tilde{\chi}_{3,4}^0} \sim M_{\tilde{\chi}_2^\pm} \sim |\mu|$, and the lightest chargino and neutralino are always a nearly mass degenerate triplet of gauginos.

- Squark masses are rather insensitive to m_0 . AMSB implies squarks and gluinos much heavier than the LSP's, completely out of reach at LEP and also at many of the proposed future colliders.
- In the slepton sector, if both the R and the L states receive the same m_0^2 contribution, the diagonal entries of the mass matrix are accidentally highly degenerate. Nearly mass degenerate and highly mixed same flavour sleptons are a distinctive feature of the minimal AMSB with a flavour independent m_0 . The lightest stau is always the lightest charged slepton. The sneutrino can be lighter than all charged sleptons, and typically the stau sneutrino is the lightest sneutrino.
- The CP-odd neutral Higgs A is usually much heavier than the Z , and the lightest CP-even neutral Higgs h^0 is analogous to the SM one [6]. Also the mass of h^0 is still more tightly bounded than in the usual SUSY scenarios, and it should lie in the range 80-120 GeV/ c^2 . Therefore, the lower limit obtained at LEP for the SM

Higgs mass already strongly constrains the AMSB parameter space. Moreover, if such a light Higgs will not be found in the first runs at the Tevatron or, further on, at the LHC, the AMSB model itself will be completely ruled out.

In the model considered here, only the slepton mass spectrum and, to some extent, the Higgs depend on the assumptions of a common scalar term m_0 . All other features are characteristics of any AMSB scenario, whatever is the procedure used to cope with the tachyonic masses of the sleptons.

Since m_0 is a free parameter, according to its value there are three possible candidates for the LSP: either the nearly mass degenerate $\tilde{\chi}_1^0/\tilde{\chi}_1^\pm$, the $\tilde{\nu}$ or the $\tilde{\tau}$. Scenarios with any of the above as LSP will be explored in the following by using the data collected by the DELPHI experiment during the period at high (LEP2) and low (LEP1) energy of the LEP operation.

3 Data and simulation samples

The results listed in this paper interpret in terms of AMSB the results of searches performed in the DELPHI experiment [7] at LEP. Those searches are described in more details in the relevant papers cited in the following sections. Some of them were used unmodified. In other cases, that are described in the following, it was necessary to adapt the original techniques to the requirements specific of the AMSB scenarios. If not otherwise specified in the text, refer to the papers cited for the description of the samples of the data and of the Standard Model background simulation used in the different analyses.

SUSYGEN [8] was used for signal simulation. As it does not allow for the calculation of the particle spectrum of the AMSB models, the input parameters were set in a way to obtain a spectrum close to the one resulting from the precise calculations in the AMSB framework of [4].

ISAJET [9], since version 7.47, allows the calculation of the particle masses and decay branching modes of the AMSB model of [3, 4] as a function of the four parameters m_0 , $m_{3/2}$, $\tan\beta$ and $sign(\mu)$. At the moment only the Leading Order (LO) corrections to the AMSB spectrum are coded in ISAJET. For a meaningful quantitative comparison with experimental results it would be advisable to use a level of precision comparable with the exact calculations [4], which could be achieved by upgrading ISAJET with Next-to-Leading Order (NLO) calculations. Therefore, in this paper, ISAJET will only be used to derive some qualitative idea on the AMSB spectra. With that limitation in mind, in section 5, as an exercise, a comparison of the experimental results with the predictions of ISAJET 7.58 (LO) is attempted.

4 Searches used to investigate the AMSB scenario

Hereafter, the possible searches able to inspect AMSB scenarios at LEP2 will be reviewed. For completeness, also few searches not fully developed will be cited. Indeed, the results of those particular searches are not supposed to be truly fundamental in constraining or testing AMSB, apart from some possible further characterization of a blind spot, eventually missed in the present scan.

4.1 LEP1 limits

The precise measurement of the Z width at LEP1 was used to put severe constraints on all possible non standard contributions. In particular, charginos with mass below $45 \text{ GeV}/c^2$ and sneutrinos with mass below $43 \text{ GeV}/c^2$ were ruled out, independently of their field composition and decay modes [10].

4.2 Search for nearly mass degenerate chargino-neutralino

One of the key features of AMSB is the very small difference between the masses of the lightest chargino and neutralino. Therefore, the results of the search for nearly mass degenerate chargino and neutralino [11] can be used to investigate AMSB.

When the masses of the lightest chargino and neutralino are very close, the visible products of the decay $\tilde{\chi}_1^\pm \rightarrow \tilde{\chi}_1^0 f f'$ (the case in which there is a sneutrino lighter than the chargino will be treated in section 4.3) carry little momentum. Therefore, they are both difficult to select and trigger on, and they can become almost undistinguishable from the huge background of two-photon events at LEP2. Dedicated techniques were used for this search.

For $\Delta M = M_{\tilde{\chi}_1^\pm} - M_{\tilde{\chi}_1^0}$ below approximately $200 \text{ MeV}/c^2$, the phase space available for the decay is limited, and the lifetime can be so long that the chargino produced at the interaction point is seen as a heavy stable charged particle in the detector, or a kink witnessing the decay can be observed in the reconstructed track. Long-lived charginos are searched for in DELPHI as single tracks with no signal (veto) in the gas or liquid radiator of the Cherenkov counter, and/or with an anomalously high ionization loss in the TPC. Kinks with both the mother chargino and the daughter charged decay particle reconstructed in the tracking devices were also searched for.

For ΔM larger than about $200 \text{ MeV}/c^2$ (or even less, in case of light sneutrinos, which tend to increase the leptonic width), the lifetime tags are no more effective. It was however observed that a high p_t photon radiated from the initial state (ISR), accompanied by few soft particles from the decay of the chargino, improves both the trigger efficiency of the signal and the rejection of the two-photon background.

Nearly mass-degenerate chargino and neutralino are possible in SUSY only if $M_2 \gg |\mu|$, that is $M_{\tilde{\chi}_1^\pm}$ and $M_{\tilde{\chi}_1^0}$ are both almost pure higgsinos, or if $M_2 \ll |\mu|$, that is $M_{\tilde{\chi}_1^\pm}$ and $M_{\tilde{\chi}_1^0}$ are both almost pure gauginos. To maximize the sensitivity to AMSB scenarios, the analysis of [11] was redone under the following assumptions:

- Only the gaugino case is of interest for AMSB.
- In the scan over the SUSY parameters, the ratio M_1/M_2 was fixed at the value of 2.8, while $\tan \beta$ was still left free to vary from 1 to 50.
- Additional scenarios with light sneutrinos were explored, besides the heavy sneutrino hypothesis already considered in [11]. Exclusion plots will be also given under the hypothesis of $100 \text{ GeV}/c^2$ sneutrinos; sneutrinos with mass between $M_{\tilde{\chi}_1^\pm} + 1 \text{ GeV}/c^2$ and $100 \text{ GeV}/c^2$; and, finally, sneutrinos lighter than $M_{\tilde{\chi}_1^\pm} + 1 \text{ GeV}/c^2$ (this case includes also all prompt chargino decays).

With respect to the results of the searches in [11], if there is a light sneutrino (either lighter than the chargino or not more than a couple of GeV/c^2 heavier) the leptonic

width gets strongly enhanced, and the lifetime shortens. In that case, the efficiencies at the smallest ΔM explored with the ISR tag, turned out to be larger than the ones computed in [11] for the same ΔM . On the other hand, as the lifetime shortens, the searches that explicitly rely on it loose efficiency.

Since there is no evidence of an excess above the Standard Model expectations, regions in the plane $(M_{\tilde{\chi}_1^\pm}, \Delta M)$ can be excluded at the 95% CL. Figures 1 and 2 show the regions excluded by the different techniques used in the search for degenerate charginos. Figure 1 (a) is the same plot with the gaugino exclusion as in [11], and includes AMSB scenarios when $M_{\tilde{\nu}} > 500 \text{ GeV}/c^2$. In figure 1 (b) the exclusion in the plane $(M_{\tilde{\chi}_1^\pm}, \Delta M)$ is computed for $M_{\tilde{\nu}} = 100 \text{ GeV}/c^2$, and therefore it holds conservatively in case of heavier sneutrinos. Figure 2 (a) was obtained with the minimal chargino cross-section (with respect to $M_{\tilde{\nu}}$) and with the lifetime corresponding to $M_{\tilde{\nu}} = M_{\tilde{\chi}_1^\pm} + 1 \text{ GeV}/c^2$. This exclusion is conservative for all AMSB scenarios with $M_{\tilde{\chi}_1^\pm} + 1 \text{ GeV}/c^2 < M_{\tilde{\nu}} < 100 \text{ GeV}/c^2$, since as $M_{\tilde{\nu}}$ increases the s - t channels interference weakens and the cross-sections gets larger; moreover, also the lifetime increases, thus improving the sensitivity of all searches for long-lived charginos. Figure 2 (b) was computed using the minimal chargino cross-section (again with respect to $M_{\tilde{\nu}}$) and for short lived charginos. It can be used to constrain AMSB scenarios with $M_{\tilde{\nu}} < M_{\tilde{\chi}_1^\pm} + 1 \text{ GeV}/c^2$ (see also section 4.3).

4.3 Search for $\tilde{\chi}_1^\pm \rightarrow \tilde{\nu} l^\pm$ decays

If the sneutrino is lighter than the chargino, the chargino decays with practically 100% branching ratio into a sneutrino and a charged lepton. Since the upper limits on the chargino cross-section in the SUGRA scenario were obtained assuming W^\pm decays for the chargino [11], they therefore cannot be translated directly into limits in AMSB scenario. Hence, only the ‘‘leptonic’’ search for charginos described in [11] was used to explore all $\Delta M_{\tilde{\nu}} = M_{\tilde{\chi}_1^\pm} - M_{\tilde{\nu}}$ larger than $3 \text{ GeV}/c^2$.

The analysis selects events with low charged multiplicity (i.e. events with no more than five reconstructed charged tracks), and without any reconstructed isolated photon. After a preselection obtained with sequential cuts, then the final selection was performed using likelihood ratio functions [12] $\mathcal{L}_R(\{x_i\})$ (one per $\Delta M_{\tilde{\nu}}$ region defined as in table 1) built as follows: for a set of variables $\{x_i\}$ (e.g visible energy, acoplanarity), the pdf’s of these variables were estimated by normalized frequency distributions for the signal (with a $\tilde{\chi}_1^0$ LSP) and the background samples. The pdf’s of these variables were denoted $f_i^S(x_i)$ for the signal events, and $f_i^B(x_i)$ for the background events that passed the same selection criteria. Six likelihood ratio functions were defined as $\mathcal{L}_R = \prod_{i=1}^n \frac{f_i^S(x_i)}{f_i^B(x_i)}$. Events with $\mathcal{L}_R > \mathcal{L}_{RCUT}$ were selected as candidate signal events. The choice of variables and the value of \mathcal{L}_{RCUT} were optimized using samples of simulated event, by minimizing the signal cross-section that was expected to be excluded at 95% confidence level in the absence of a signal. This procedure was repeated for every investigated centre-of-mass energy. Basically after the final selection, the remaining set of events consisted of low multiplicity events with high acoplanarity and high missing energy.

In the present search, new limits were set using only efficiencies computed with fully leptonic decays events selected by the fully leptonic selections, and without considering events with cascade decays (i.e. $\tilde{\chi}_1^\pm \rightarrow \tilde{\chi}_2^0 X \rightarrow \tilde{\chi}_1^0 X X'$) allowed in the SUGRA model but forbidden in AMSB.

$\langle E_{cm} \rangle$ (GeV)	191.6	195.6	199.6	201.7	204.9	206.7	208.2	207*
$\int \mathcal{L}$ (pb ⁻¹)	25.8	76.8	84.3	40.5	78.3	78.8	7.2	60.2
	$3 \leq \Delta M_{\tilde{\nu}} < 5 \text{ GeV}/c^2$							
Data	2	13	17	7	8	11	1	10
MC	6.0 ^{+0.7} _{-0.4}	17.4 ^{+1.9} _{-1.2}	17.9 ^{+1.7} _{-1.2}	8.7 ^{+0.8} _{-0.6}	9.8 ^{+1.3} _{-0.8}	9.9 ^{+1.3} _{-0.8}	0.9 ^{+0.1} _{-0.1}	18.8 ^{+1.5} _{-1.1}
	$5 \leq \Delta M_{\tilde{\nu}} < 10 \text{ GeV}/c^2$							
Data	2	2	4	5	0	0	0	4
MC	1.3 ^{+0.4} _{-0.2}	3.8 ^{+1.1} _{-0.5}	4.2 ^{+1.0} _{-0.4}	2.1 ^{+0.5} _{-0.2}	1.0 ^{+0.7} _{-0.2}	1.0 ^{+0.7} _{-0.2}	0.1 ^{+0.1} _{-0.1}	3.6 ^{+0.8} _{-0.4}
	$10 \leq \Delta M_{\tilde{\nu}} < 25 \text{ GeV}/c^2$							
Data	1	5	7	1	5	3	0	3
MC	1.6 ^{+0.4} _{-0.1}	5.0 ^{+1.0} _{-0.3}	5.1 ^{+0.9} _{-0.3}	2.5 ^{+0.5} _{-0.2}	3.7 ^{+0.8} _{-0.3}	3.7 ^{+0.8} _{-0.3}	0.3 ^{+0.1} _{-0.1}	2.3 ^{+0.6} _{-0.2}
	$25 \leq \Delta M_{\tilde{\nu}} < 35 \text{ GeV}/c^2$							
Data	2	11	5	3	5	8	0	3
MC	2.8 ^{+0.4} _{-0.2}	9.0 ^{+1.1} _{-0.4}	8.5 ^{+0.9} _{-0.3}	4.1 ^{+0.5} _{-0.2}	5.5 ^{+0.8} _{-0.3}	5.6 ^{+0.8} _{-0.3}	0.5 ^{+0.1} _{-0.1}	5.3 ^{+0.7} _{-0.2}
	$35 \leq \Delta M_{\tilde{\nu}} < 50 \text{ GeV}/c^2$							
Data	6	20	10	4	11	10	2	10
MC	5.5 ^{+0.4} _{-0.2}	16.0 ^{+1.1} _{-0.5}	15.5 ^{+0.9} _{-0.4}	7.3 ^{+0.5} _{-0.2}	12.8 ^{+0.8} _{-0.3}	12.9 ^{+0.8} _{-0.3}	1.2 ^{+0.1} _{-0.1}	11.7 ^{+0.7} _{-0.3}
	$50 \text{ GeV}/c^2 \leq \Delta M_{\tilde{\nu}}$							
Data	9	32	14	5	22	18	0	16
MC	8.4 ^{+0.5} _{-0.2}	23.8 ^{+1.2} _{-0.6}	24.0 ^{+1.1} _{-0.5}	11.5 ^{+0.6} _{-0.3}	18.6 ^{+0.8} _{-0.3}	18.7 ^{+0.8} _{-0.3}	1.7 ^{+0.1} _{-0.1}	14.2 ^{+0.6} _{-0.3}
	TOTAL (logical .OR. between different $\Delta M_{\tilde{\nu}}$ windows)							
Data	10	52	34	13	37	36	3	31
MC	15.7 ^{+0.8} _{-0.5}	46.2 ^{+2.2} _{-1.6}	43.9 ^{+1.9} _{-1.3}	21.2 ^{+0.9} _{-0.7}	33.2 ^{+1.5} _{-1.0}	33.4 ^{+1.5} _{-0.9}	3.1 ^{+0.1} _{-0.1}	38.8 ^{+1.7} _{-1.2}

Table 1: The number of events observed in data and the expected number of background events in the search for chargino decaying into a sneutrino and a charged lepton, at the centre-of-mass energies collected by DELPHI in 1999 and 2000. In the last column there are the data collected in year 2000 with the TPC not fully operational, considered at their mean centre-of-mass energy

Table 1 summarizes the number of events observed and expected, and the luminosities used at the different centre-of-mass energies. The data collected during year 2000 with and without the TPC fully operational (see [11]) were treated as different channel in the analysis. No excess was observed above the SM expectations.

The efficiencies at the centre-of-mass energy of 208 GeV of the fully leptonic selection are plotted in figure 3 (a) as function of the chargino and sneutrino masses. Since up to five visible charged particles were allowed and no leptonic identification was required, those efficiencies had only very little dependence on the flavour of the charged lepton in the final state. The efficiencies of figure 3 (a) were computed using events simulated with three body $\tilde{\chi}_1^+ \rightarrow l^+ \nu \tilde{\chi}_1^0$ decays. It was indeed verified with some samples of fully simulated events with the two body decay $\tilde{\chi}_1^+ \rightarrow l^+ \tilde{\nu}$ searched for in AMSB, that the efficiencies used in the analysis were always not larger than the ones expected for the two body decays (in fact, given the momentum of the visible charged particles which is in mean larger in the two body sample than in the three body one, the efficiency used was always smaller than the one expected for the true signal with two body decay, especially at the lowest $\Delta M_{\tilde{\nu}}$ inspected). Therefore, the limits obtained are not overestimated, and possibly conservative at small $\Delta M_{\tilde{\nu}}$.

There was no evidence of excess above the SM expectations: figure 3 (b) displays the 95% CL upper limit of the chargino cross-section at the reference centre-of-mass energy of 208 GeV, as function of the masses of the chargino and of the sneutrino. If that exclusion is compared with the theoretical expectation of the same cross-section (in figure 3 (c) is shown the minimal expected $e^+e^- \rightarrow \tilde{\chi}_1^+ \tilde{\chi}_1^-$ cross-section, as function of $M_{\tilde{\chi}_1^\pm}$), one can exclude a region in the plane $(M_{\tilde{\chi}_1^\pm}, M_{\tilde{\nu}}$) at the same confidence level: the excluded region is shown in figure 3 (d).

The exclusion when $0 < \Delta M_{\tilde{\nu}} < 3 \text{ GeV}/c^2$, as obtained with the results of the search for nearly mass degenerate charginos, can be derived from figure 2 (b), by simply substituting ΔM with $\Delta M_{\tilde{\nu}}$ in the y axis. The same observation on the conservativeness of the limits obtained when the chargino decays into two bodies and the efficiencies are estimated from samples of three body decays also holds for the search at $\Delta M_{\tilde{\nu}} < 3 \text{ GeV}/c^2$. For $M_{\tilde{\chi}_1^\pm} < 54 \text{ GeV}/c^2$, only a narrow band that corresponds to $0 < \Delta M_{\tilde{\nu}} < 200 \text{ MeV}/c^2$ cannot be excluded, at present, by the DELPHI results.

If also the stau, or some other charged slepton, has a mass which is intermediate between the mass of the chargino and that of the sneutrino, figure 3 (b) should be intended as the 95% CL upper limit of the chargino cross-section times its branching ratio into $l^\pm \tilde{\nu}$.

4.4 Search for $e^+e^- \rightarrow \tilde{\chi}_1^0 \tilde{\chi}_2^0$

Searches for $\tilde{\chi}_1^0 \tilde{\chi}_2^0$ production with $\tilde{\chi}_2^0 \rightarrow q\bar{q}\tilde{\chi}_1^0$, $\tilde{\chi}_2^0 \rightarrow \mu^+ \mu^- \tilde{\chi}_1^0$, $\tilde{\chi}_2^0 \rightarrow e^+ e^- \tilde{\chi}_1^0$, $\tilde{\chi}_2^0 \rightarrow Z\tilde{\chi}_1^0$, and $\tilde{\chi}_2^0 \rightarrow \tilde{\tau}\tau$ decays have been presented in [11]. Limits for production cross-section times branching ratio to the corresponding final state ranged typically from 0.05 pb to 0.2 pb, depending primarily on $M_{\tilde{\chi}_2^0} - M_{\tilde{\chi}_1^0}$.

Since in AMSB $M_1/M_2 \sim 2.8$, and $M_{\tilde{\chi}_1^0} \sim M_{\tilde{\chi}_1^\pm} \sim M_2$ and $M_{\tilde{\chi}_2^0} \sim M_1$, there is relatively little room for the production of $\tilde{\chi}_1^0 \tilde{\chi}_2^0$ at the LEP energies. Indeed, only if $\tilde{\chi}_1^0$ is sufficiently light a $\tilde{\chi}_2^0$ almost three times as heavy can be produced in association, as $M_{\tilde{\chi}_1^0} + M_{\tilde{\chi}_2^0}$ must be below \sqrt{s} . In that case, the $\tilde{\chi}_2^0$ decays mainly to $\tilde{\chi}_1^0 Z$ and $\tilde{\chi}_1^\pm W^\mp$ [9]. For the $\tilde{\chi}_2^0 \rightarrow \tilde{\chi}_1^0 Z$ decay, the results of the neutralino searches presented in [11] can be directly used. Since in AMSB scenarios the chargino is nearly mass degenerate with the neutralino, the decay $\tilde{\chi}_2^0 \rightarrow \tilde{\chi}_1^\pm W^\mp$, with $\tilde{\chi}_1^\pm \rightarrow \pi^\pm \tilde{\chi}_1^0$ and $W \rightarrow q\bar{q}'$, results in the same final state as $\tilde{\chi}_2^0 \rightarrow \tilde{\chi}_1^0 q\bar{q}'$. Also in this case, limits on $\tilde{\chi}_1^0 \tilde{\chi}_2^0$ production with the above final state presented in [11] can be used. Indeed, when the W decays leptonically, the visible objects in the final states are different from those of the standard search for neutralinos, because of the soft particle coming out from the chargino decay, which can be relevant in a low multiplicity environment. A dedicated search is needed, not included in this paper.

If there are sleptons with a mass between $M_{\tilde{\chi}_1^0}$ and $M_{\tilde{\chi}_2^0}$, cascade decays of $\tilde{\chi}_2^0$ ($\tilde{\chi}_2^0 \rightarrow \tilde{\ell}l$, $\tilde{\ell} \rightarrow \tilde{\chi}_1^0 \bar{l}$) can take place. In this case there are two mass differences ($\Delta M_{\tilde{\ell}}$) characterizing the process: $M_{\tilde{\chi}_2^0} - M_{\tilde{\ell}}$ and $M_{\tilde{\ell}} - M_{\tilde{\chi}_1^0}$. It was verified that if $\tilde{\ell} = (\tilde{\mu}, \tilde{e})$ the results of the searches for $e^+e^- \rightarrow \tilde{\chi}_2^0 \tilde{\chi}_1^0$, where $\tilde{\chi}_2^0 \rightarrow \mu^+ \mu^- \tilde{\chi}_1^0$ or $\tilde{\chi}_2^0 \rightarrow e^+ e^- \tilde{\chi}_1^0$, can be used, provided that from the $\Delta M_{\tilde{\ell}}$ definitions above the one giving the more conservative result is used in place of $M_{\tilde{\chi}_2^0} - M_{\tilde{\chi}_1^0}$.

For $\tilde{\tau}_1$ as the intermediate slepton, the tau cascade search described in [11] was studied in a wider range of $M_{\tilde{\tau}_1} - M_{\tilde{\chi}_1^0}$. The tau cascade search is sensitive to $\tilde{\chi}_1^0 \tilde{\chi}_2^0$ production with $\tilde{\chi}_2^0 \rightarrow \tilde{\tau}\tau$ and $\tilde{\tau} \rightarrow \tilde{\chi}_1^0 \tau$, where the second τ produced has very low energy. At the preselection level, well reconstructed low multiplicity events with missing energy, missing

mass, and no more than two reconstructed jets were selected. In particular, the total visible energy including badly reconstructed tracks was required to be less than 140 GeV, the number of charged particles was required to be at least two and at most eight, and events with more than four neutral particles were rejected. Two or more of the charged particles also had to satisfy stricter criteria on reconstruction and impact parameters. Having had no evidence of excesses above the SM expectations after the selection (see [11]), the resulting cross-section limits are shown in figure 4.

Light sneutrinos lead to an undetectable $\tilde{\chi}_2^0 \rightarrow \tilde{\nu}\bar{\nu}$ and $\tilde{\nu} \rightarrow \tilde{\chi}_1^0\nu$ decay chain.

4.5 Search for a charged slepton as the LSP

It is rather unlikely that a stau (or another charged slepton) is the LSP in the AMSB. In a scan of the parameter space performed with ISAJET [9] no points were obtained with $M_{\tilde{\chi}_1^0} > M_{\tilde{\tau}}$. However, the calculations in [4] still allow some corner in the space of the AMSB parameters with the $\tilde{\tau}_1$ being the LSP. In that case, if R-parity is conserved, the stau must be stable. The DELPHI results of the search for heavy stable charged particles were already presented in [13], together with the description of the method used in the analysis.

Staus are expected to be almost maximally mixed in AMSB [4]. Reference [13] showed that, the results of the search for heavy stable charged particles in DELPHI can exclude a stable $\tilde{\tau}_1$ with mass below 96 GeV/ c^2 at the 95% CL, even at the level of mixing that gives the lowest $\tilde{\tau}_1^+\tilde{\tau}_1^-$ production cross-section,

4.6 Search for cascades from sleptons

Considering that the decay $\tilde{l}^\pm \rightarrow \tilde{\chi}_1^\pm\nu_l$ is practically invisible, due to the softness of the visible decay products of the chargino, the only cascades originating from a charged slepton (namely, a stau) in AMSB that can be taken into account are:

- $\tilde{\tau}_1 \rightarrow \tilde{\chi}_1^0\tau$, the same channel searched for in MSSM (see results on [11]);
- $\tilde{\tau}_1 \rightarrow \tilde{\nu}_\tau f f'$, with visible final states that can be similar to the chargino ones.

In the case of the sneutrino production, the decay $\tilde{\nu} \rightarrow \tilde{\chi}_1^0\nu$ is clearly invisible. On the other hand, $\tilde{\nu} \rightarrow \tilde{\chi}_1^\pm l^\mp$ can be observed, probably with similar techniques as those used in the usual searches for sleptons.

Those cascades were not fully studied for this paper, although approximate limits on cross-section times branching ratio could be derived analyzing the results of the searches for “standard” charginos and sleptons.

4.7 Search for the Higgs boson in AMSB

Since in AMSB $m_A \gg m_Z$, the lightest supersymmetric neutral Higgs h^0 behaves like the SM Higgs boson, and the limits obtained on the mass of the Higgs in the SM can be translated into the same lower limits on the mass of the h^0 in AMSB, provided that the decay branching fractions of the Higgs into supersymmetric particles are small.

If $m_A \gg m_Z$, h^0 can be produced at LEP only in association with the Z (higgsstrahlung), and with the same cross-section as in the SM. When there are SUSY particles

lighter than $m_{h^0}/2$, also decays of the Higgs into those particles are allowed. This is the case of AMSB, when there are light winos, sneutrinos or charged sleptons. Possible SUSY decays of the h^0 are:

- $h^0 \rightarrow \tilde{\chi}_1^0 \tilde{\chi}_1^0, \tilde{\chi}_1^+ \tilde{\chi}_1^-, \tilde{\nu} \tilde{\nu}$, all invisible or practically invisible in AMSB, apart from some possible cascades;
- $h^0 \rightarrow \tilde{l}^+ \tilde{l}^-$, the visibility of which depends on the mass difference between the slepton and the LSP.

The DELPHI bound on the SM Higgs mass is $M_H > 114.3 \text{ GeV}/c^2$ at the 95% CL [14]. DELPHI measured also the limit on the production cross-section of an invisibly decaying Higgs boson [15]. Assuming a 100% BR into invisible particles, DELPHI can exclude Higgs masses below $113.0 \text{ GeV}/c^2$. Figure 8 of reference [15] shows how the limit on the mass of the lightest supersymmetric Higgs boson depends on the branching fraction into invisible states, assuming that all other decay modes are the SM ones: that limit starts from $114.3 \text{ GeV}/c^2$ when $\text{BR}(h^0 \rightarrow \text{inv.}) = 0$ (that is, the h^0 decays according the SM) and $113.0 \text{ GeV}/c^2$ when $\text{BR}(h^0 \rightarrow \text{inv.}) = 1$. The same limits on m_{h^0} apply in AMSB, provided there are no visible SUSY decays with sizeable branching fractions.

5 Constraints to the AMSB spectrum

The negative results of the searches described in this paper were used to constrain the AMSB parameter space. To do that, the experimental exclusions measured were compared with the mass spectra produced by ISAJET 7.58 [9]. A scan over the AMSB parameters was done by varying them in the following ranges: $2 < m_{3/2} < 50 \text{ TeV}/c^2$ at steps of $1.5 \text{ TeV}/c^2$; $40 < m_0 < 1000 \text{ GeV}/c^2$ at steps of $10 \text{ GeV}/c^2$ if m_0 was below $600 \text{ GeV}/c^2$, $50 \text{ GeV}/c^2$ otherwise; $1.5 < \tan \beta < 40.5$ at steps of 1 if $\tan \beta < 10$, steps of 5 otherwise; both positive and negative μ .

Figure 5 shows, on top, the points in the plane $(m_0, m_{3/2})$ generated with ISAJET. The region of the space with no points in that plot were considered as not allowed by the program, because some of the sparticle masses would result to be tachyonic. One can notice that this imply a certain degree of correlation between m_0 and $m_{3/2}$, since by cutting away slices at low $m_{3/2}$ also the value of the lowest admissible m_0 gets increased. In the middle plot are shown the points that remained after the application of the model independent bounds on the chargino and sneutrino masses obtained at LEP1. In the lower part of the figure are plotted instead the points that remained after having applied all the results of the searches described in this paper.

Since in AMSB the Higgs is preferably light, the most of the exclusion in the space of the AMSB parameters was given exactly by the negative results of the searches for the SM and the invisible Higgs. The negative results of the other searches could enlarge further the rejection especially at low $m_{3/2}$ (chargino searches) and low m_0 (searches with sleptons). The effect of the search for the standard and invisible Higgs can be evaluated in figure 6. In that figure, the plot labelled “AMSB” shows all the points generated with ISAJET in the plane $(m_h, \tan \beta)$. On its right (“LEP1”) one can see all the points remained in that plane after the LEP1 chargino and sneutrino exclusions. Below, the plot on the left shows the points that still survived after the negative results of the SM and invisible Higgs searches

in DELPHI. After that stage, still some point with $m_h < 114 \text{ GeV}/c^2$ cannot be excluded, because of the presence of light SUSY particles that give rise to unexplored topologies in the Higgs boson decay. However, the remaining plot of the figure (“LEP2”) shows that, after having applied the full set of results presented in this paper to constrain AMSB, no point survived with a mass of the lightest Higgs below the SM limit of $114.3 \text{ GeV}/c^2$.

It is interesting to observe the impact of the searches for AMSB on some particle masses. Figure 7 shows the number of points generated by ISAJET and passing the three steps of selection as in figure 5, as a function of the mass of the lightest neutralino and of the lightest sneutrino. It turned out at the end that neutralinos lighter than approximately $70 \text{ GeV}/c^2$ and sneutrinos lighter than $100 \text{ GeV}/c^2$ should not be allowed in AMSB.

In ISAJET the AMSB spectra are computed at the LO only, and the outcomes of this exercise must be considered at the moment just as qualitative results. Moreover, it should be checked more carefully whether the small blind spots that exist in some of the analyses used were not missed by chance only because of the rough granularity of the scan.

Having all those caveats in mind, one can just continue with the exercise, and notice that, whenever those findings would be confirmed even using NLO calculation to compare with the data, the possible AMSB explanation for a light sneutrino ($M_{\tilde{\nu}}$ less than about $80 \text{ GeV}/c^2$), suggested to cure some of the discrepancies in the fit of the precision electroweak data [16], could be ruled out by the results of the searches for AMSB scenarios in DELPHI.

6 Conclusions

A compilation of preliminary results of the searches performed with the data collected with the DELPHI detector at LEP, and relevant to explore AMSB scenarios, was presented. An interpretation of the limits obtained in searches motivated by other SUSY breaking scenarios was presented, whenever appropriate. Some of the searches were indeed developed specifically to improve the sensitivity to AMSB. There was no evidence for a signal beyond the Standard Model, and limits were set on the sparticle production in the AMSB framework.

Such a collection of results can be relevant in itself and can provide phenomenologists with the experimental input needed to carefully test the model. As an illustration of the possible tests of AMSB that can be performed once accurate calculations of sparticle spectra will be available, the limits on sparticle production were translated using the LO calculations, to constraints on the space of the AMSB parameters and on the mass spectrum of the lightest SUSY particles of the model.

Acknowledgements

We thank Gian Giudice for the valuable comments and suggestions that helped us in interpreting the experimental results within the AMSB phenomenology.

References

- [1] A.H. Chamseddine, R. Arnowitt, P. Nath, Phys. Rev. Lett. **49** (1982) 970;
R. Barbieri, S. Ferrara, C.A. Savoy, Phys. Lett. **B119** (1982) 343.
- [2] M. Dine, A.E. Nelson, Phys. Rev. **D48** (1993) 1277;
M. Dine, A.E. Nelson, Y. Shirman, Phys. Rev. **D51** (1995) 1362;
M. Dine, A.E. Nelson, Y. Nir, Y. Shirman, Phys. Rev. **D53** (1996) 2658.
- [3] L. Randall, R. Sundrum, Nucl. Phys. **B557** (1999) 79.
- [4] G.F. Giudice, M. Luty, H. Murayama, R. Rattazzi, JHEP **98** (1998) 12;
T. Gherghetta, G.F. Giudice, J.D. Wells, Nucl. Phys. **B559** (1999) 27;
J. L. Feng, T. Moroi, Phys. Rev. **D61** (2000) 095004.
- [5] A. Pomarol, R. Rattazzi, JHEP **99** (1999) 5.
- [6] S. Su, Nucl. Phys. **B573** (2000) 87.
- [7] DELPHI Coll., P. Aarnio *et al.*, Nucl. Instr. and Meth. **303** (91) 233;
DELPHI Coll., P. Abreu *et al.*, Nucl. Instr. and Meth. **378** (96) 57.
- [8] S. Katsanevas and P. Morawitz, Comp. Phys. Comm. **112** (98) 227.
- [9] H. Baer, F.E. Paige, S.D. Protopopescu, X. Tata, "Simulating Supersymmetry with ISAJET 7.0/ISASUSY 1.0", Published in Argonne Accel. Phys. 1993:0703-720.
- [10] Particle Data Group, D. Groom, *et al.*, E. Phys. J. **C15** (2000) 1
- [11] J. Abdallah, *et al.*, DELPHI 2001-085 CONF 513, EPS 333 - LP01 145.
- [12] T.W. Anderson, An Introduction to multivariate analysis, New York Wiley, 1958.
- [13] R. Alemany, E. Anashkin, F. Cavallo, P. Checchia, C. Garcia, F. Navarra, F. Mazzucato, E. Piotto, U. Schwickerath, DELPHI 2001-075 CONF 503.
- [14] DELPHI Coll., P. Abreu *et al.*, Phys. Lett. **B499** (2001) 23.
- [15] M. Stanitzki, A. Sopczak, G. Gomez-Ceballos, F. Matorras, DELPHI 2001-079 CONF 507, EPS 327 - LP01 140.
- [16] G. Altarelli, F. Caravaglios, G.F. Giudice, P. Gambino, G. Ridolfi, JHEP **106** (2001) 18.

DELPHI PRELIMINARY

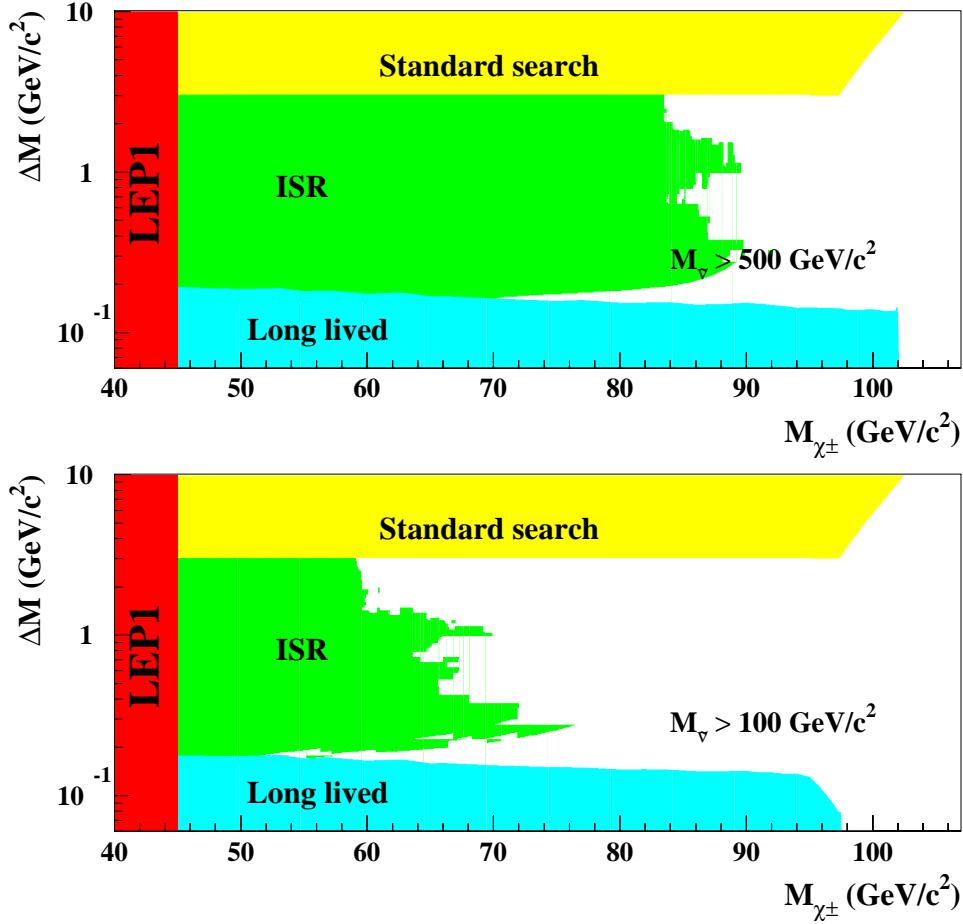


Figure 1: Regions in the plane $(M_{\chi_{\pm}}, \Delta M = M_{\chi_{\pm}} - M_{\chi_1^0})$ excluded by DELPHI at the 95% CL when the chargino is gaugino-like, as in AMSB. The standard search for high ΔM charginos, the search for soft particles accompanied by ISR, and the search for long-lived charginos were used. The scenarios in the two plots are: (a) $M_{\tilde{\nu}} > 500 \text{ GeV}/c^2$; (b) $M_{\tilde{\nu}} > 100 \text{ GeV}/c^2$.

DELPHI PRELIMINARY

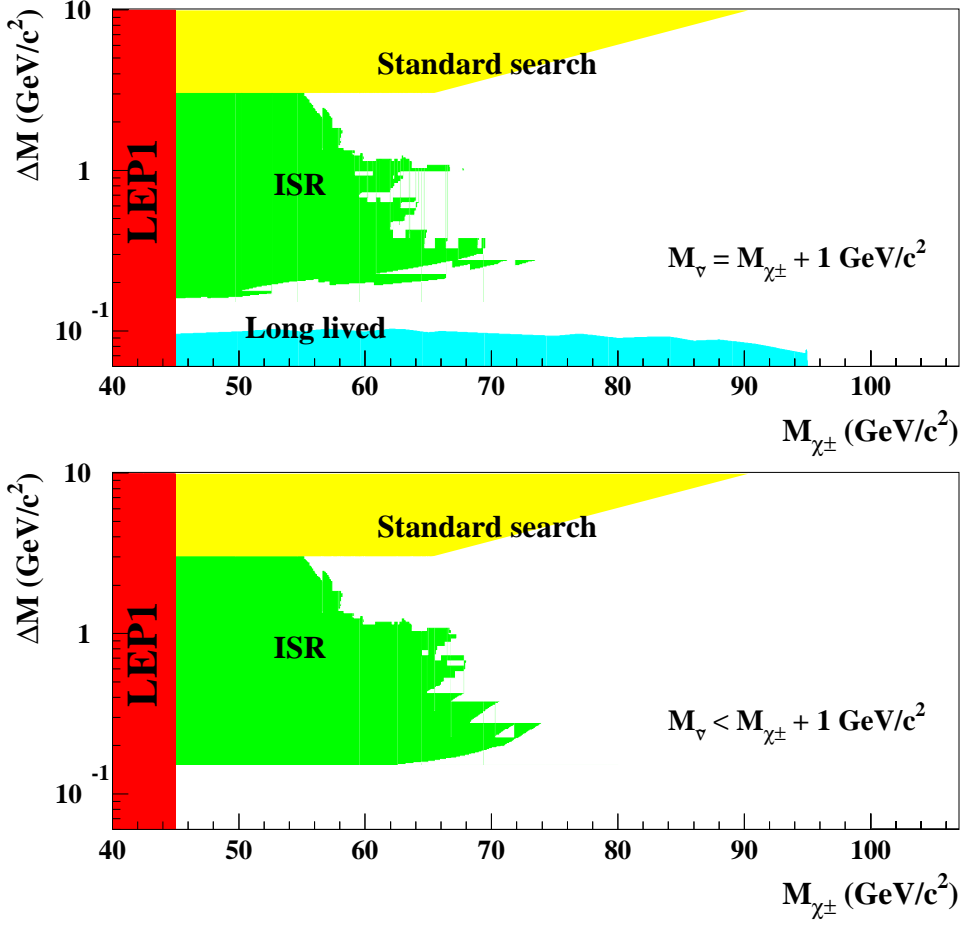


Figure 2: Regions in the plane $(M_{\tilde{\chi}_1^\pm}, \Delta M = M_{\tilde{\chi}_1^\pm} - M_{\tilde{\chi}_1^0})$ excluded by DELPHI at the 95% CL when the chargino is gaugino-like, as in AMSB. The standard search for high ΔM charginos, the search for soft particles accompanied by ISR, and the search for long-lived charginos were used. The scenarios in the two plots are: (a) $M_{\tilde{\nu}} \geq M_{\tilde{\chi}_1^\pm} + 1 \text{ GeV}/c^2$ (still flying charginos); (b) $M_{\tilde{\nu}} < M_{\tilde{\chi}_1^\pm} + 1 \text{ GeV}/c^2$ (short lived charginos).

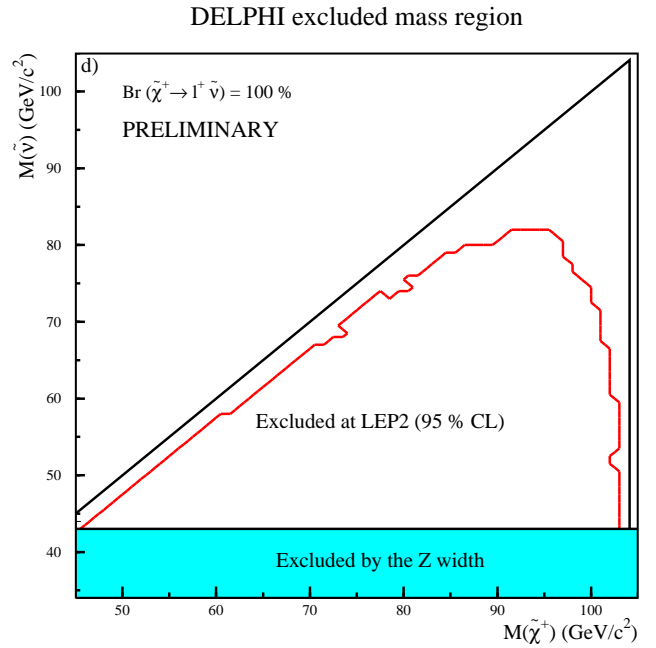
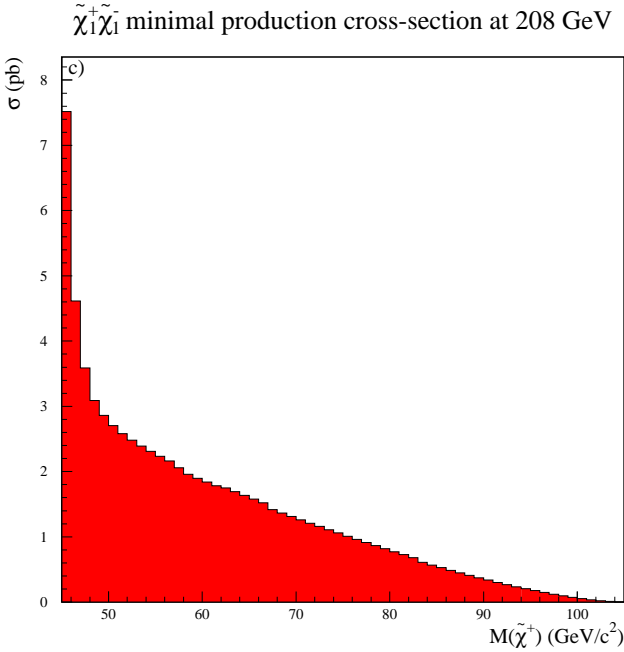
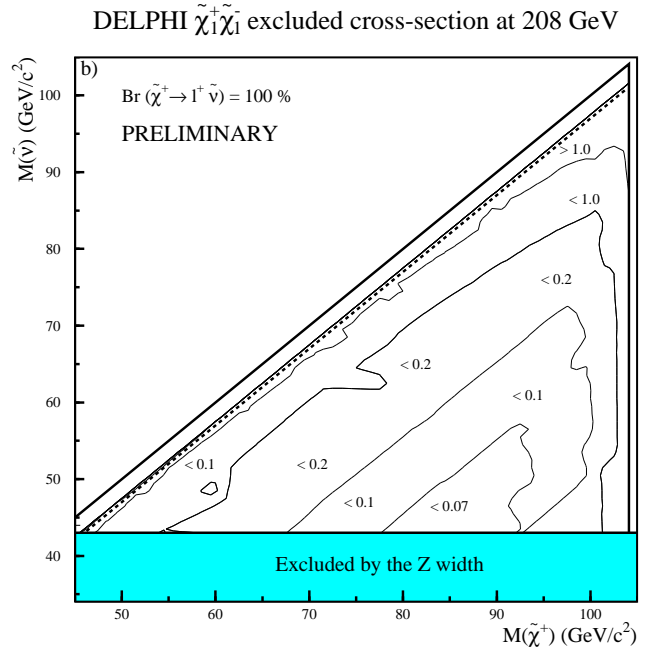
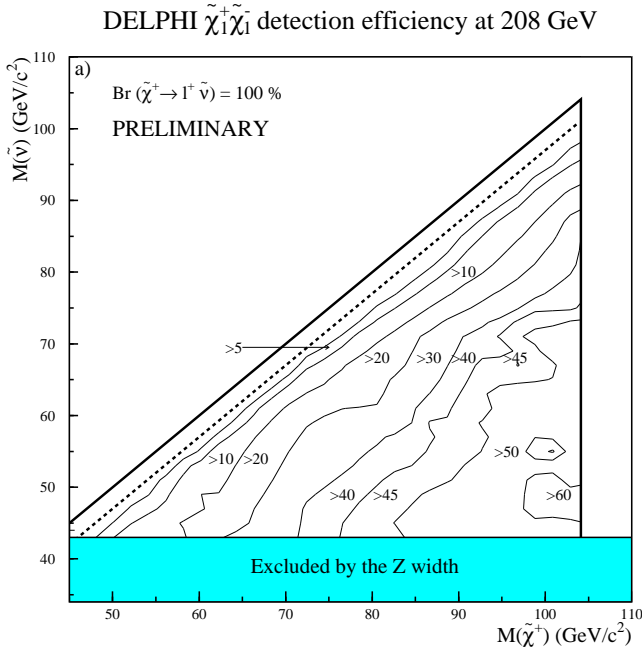


Figure 3: a) Chargino pair production detection efficiencies (%) for the fully leptonic decay channel at $\sqrt{s}=208$ GeV in the $(M_{\tilde{\chi}_1^\pm}, M_{\tilde{\nu}}$) plane; a 100% BR of $\tilde{\chi}_1^\pm \rightarrow \tilde{\nu}l^\pm$ is assumed. b) Equivalent excluded cross-section at 208 GeV. c) Minimal, with respect to $M_{\tilde{\nu}}$, $e^+e^- \rightarrow \tilde{\chi}_1^+ \tilde{\chi}_1^-$ cross-section in AMSB, as function of the mass of the chargino. d) Region excluded in the plane $(M_{\tilde{\chi}_1^\pm}, M_{\tilde{\nu}})$ by the search described in the text. Sneutrinos lighter than $43 \text{ GeV}/c^2$ were already excluded at LEP1.

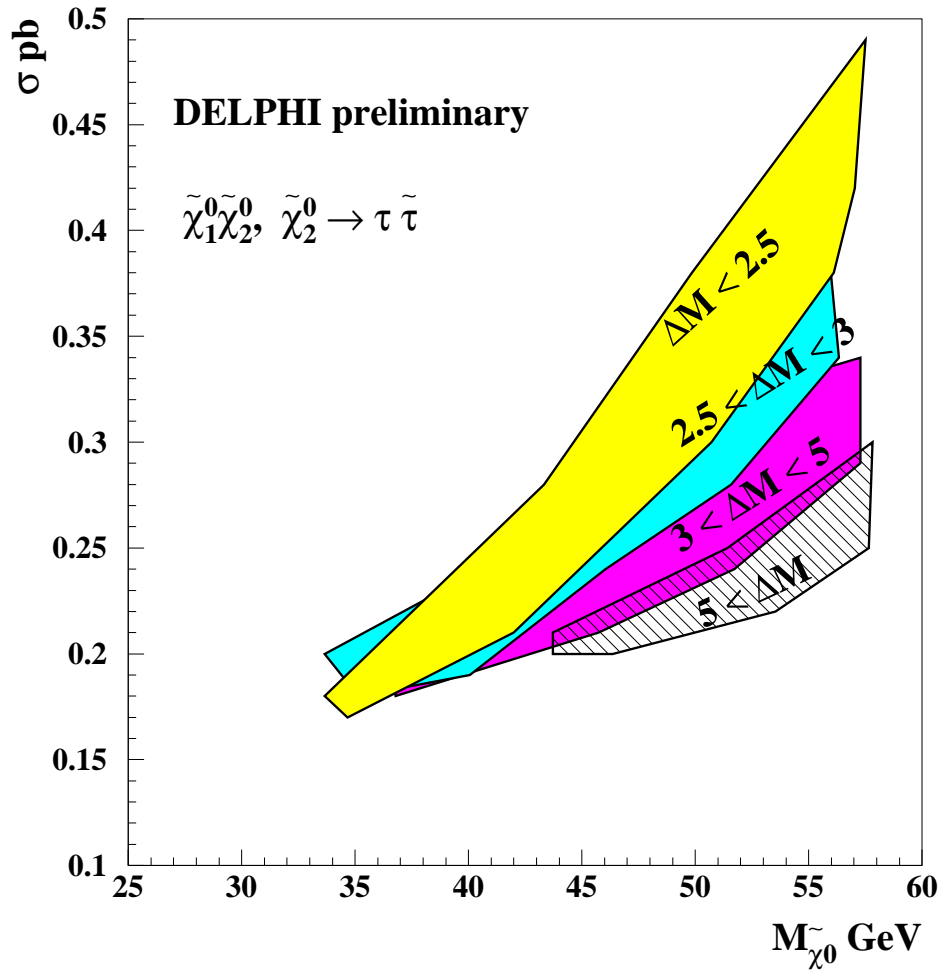


Figure 4: Cross-section limits for the $\tilde{\chi}_1^0 \tilde{\chi}_2^0$ production when $\tilde{\chi}_2^0$ decays entirely to $\tilde{\tau}_1 \tau$. The limits are shown for several ranges of $\Delta M = M_{\tilde{\tau}_1} - M_{\tilde{\chi}_1^0}$. The widths of the bands are due to dependence of the limit on ΔM and to statistical fluctuations of the efficiency due to limited Monte Carlo statistics.

DELPHI PRELIMINARY

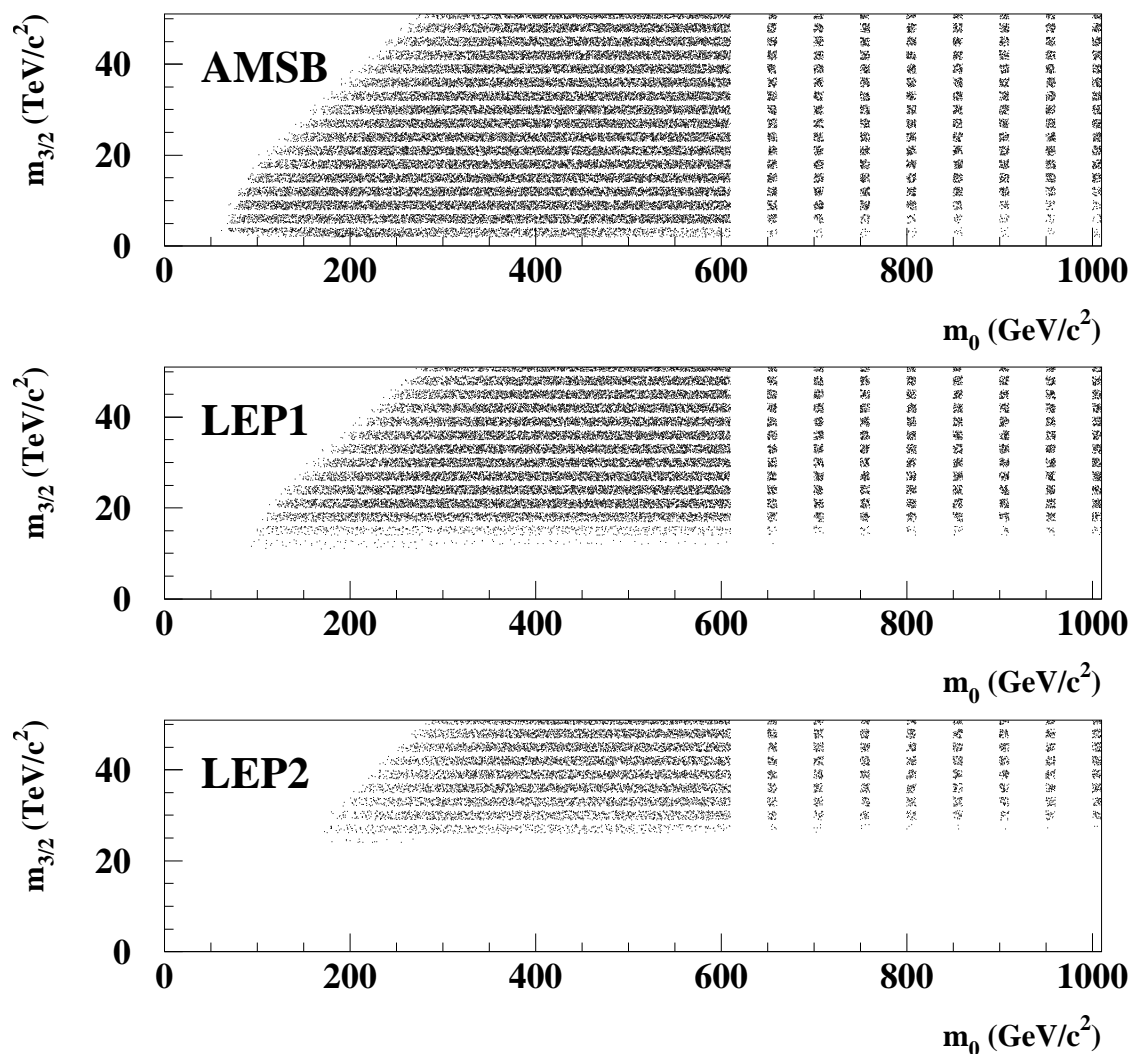


Figure 5: On top, physically allowed m_0 and $m_{3/2}$ parameters in AMSB, as obtained in a scan of the AMSB parameter space with ISAJET, as described in the text. In the middle, the points that remained after having applied the chargino and sneutrino mass bound of LEP1. Below, the set of points from the scan remaining after having considered all the results of the searches described in this work.

DELPHI PRELIMINARY

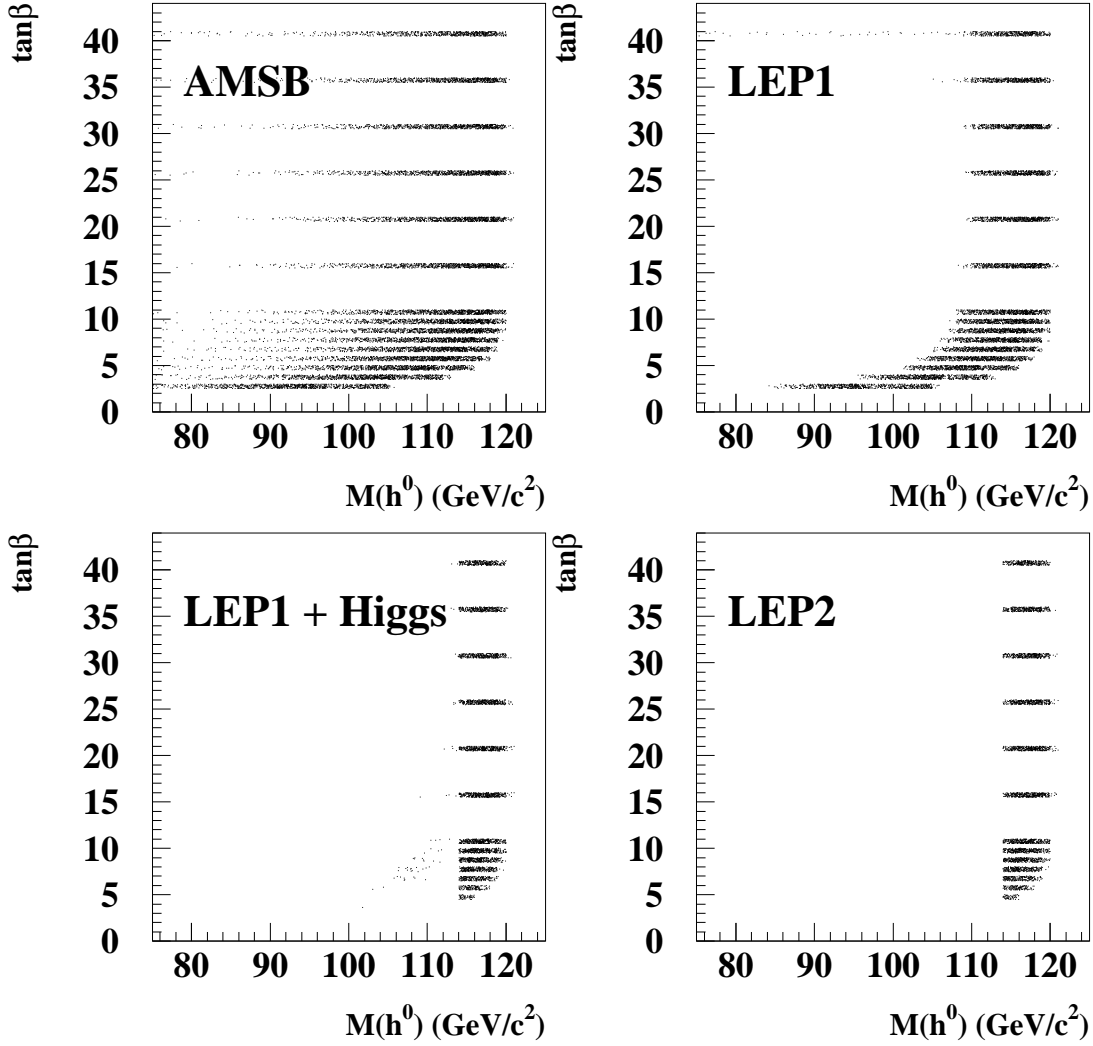


Figure 6: Top, left: physically allowed M_h and $\tan\beta$ in AMSB, as obtained in a scan of the AMSB parameter space with ISAJET, as described in the text. Top, right: the points that remained after having applied the chargino and sneutrino mass bound of LEP1. Bottom, left: the points still survived after the negative results of the searches for the SM and invisible Higgs bosons. Bottom, right: the set of points remaining finally after having considered all the results of the searches described in this work. No points survived for which $M_h < 114.3$ GeV/c².

DELPHI PRELIMINARY

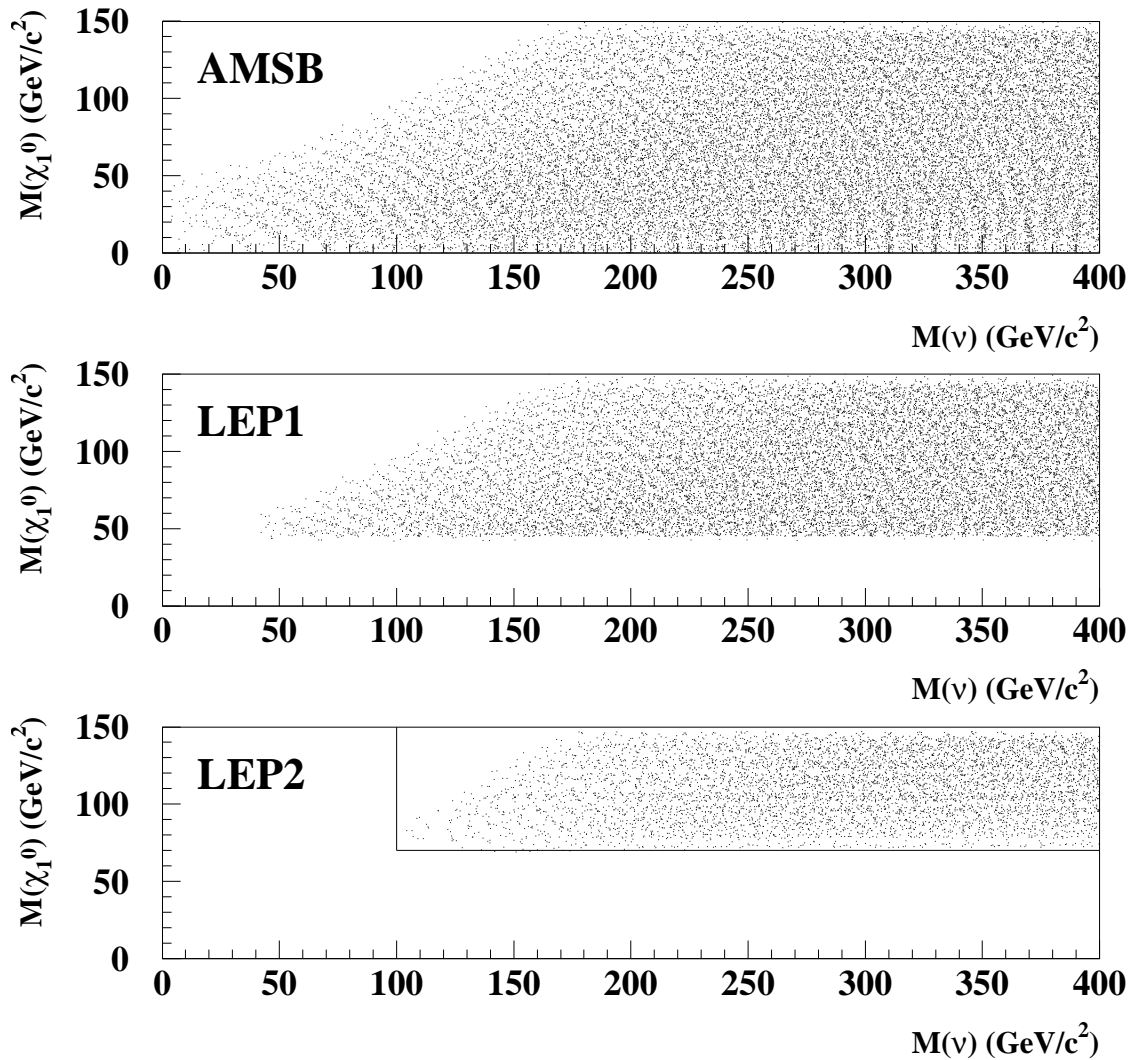


Figure 7: On top, physically allowed $M_{\tilde{\chi}_1^0}$ and $M_{\tilde{\nu}}$ in AMSB, as obtained in a scan of the AMSB parameter space with ISAJET, as described in the text. In the middle, the points that remained after having applied the chargino and sneutrino mass bound of LEP1. Below, the set of points from the scan remaining after having considered all the results of the searches described in this work. No points survived for which $M_{\tilde{\chi}_1^0} < 70$ GeV/c² or $M_{\tilde{\nu}} < 100$ GeV/c².